Published by Elsevier Inc.

ISSN 0735-1097/04/$30.00
doi:10.1016/j.jacc.2004.01.051

Electrophysiologic Properties of Pulmonary Veins Assessed Using a Multielectrode Basket Catheter

Koichiro Kumagai, MD, FACC, Masahiro Ogawa, MD, Hiroo Noguchi, MD, Tomoo Yasuda, MD, Hideko Nakashima, MD, Keijiro Saku, MD, FACC

Fukuoka, Japan

OBJECTIVES The purpose of the present study was to evaluate the electrophysiologic properties within the pulmonary vein (PV) and at the PV–left atrial (LA) junction.

BACKGROUND It has been recognized that atrial fibrillation (AF) can originate from PVs. However, the electrophysiologic properties of the PV have not been well characterized.

METHODS Thirty-two bipolar electrograms were recorded simultaneously from a basket catheter placed in 81 PVs of 48 patients with paroxysmal AF. The programmed stimulation was performed in the distal PV and PV-LA junction. Activation maps of PVs were analyzed from episodes of spontaneous onset of AF and initiation of induced AF by a single extrastimulus.

RESULTS The effective refractory period (ERP) of the distal PV was significantly shorter than that of the PV-LA junction (177 ± 43 vs. 222 ± 30 ms, $p < 0.0001$). The conduction delay from the distal PV to the PV-LA junction was significantly longer than that from the PV-LA junction to distal PV (73 ± 40 vs. 32 ± 17 ms, $p < 0.0001$). During initiation of AF, a short coupled extrastimulus or rapid, repetitive focal activities originating from the PV formed a PV-LA reciprocating re-entrant circuit involving exit and entrance breakthrough points at the PV-LA junction. Also, an unstable re-entrant circuit within the PV was observed.

CONCLUSIONS The presence of ERP heterogeneity and anisotropic conduction properties within the PV and at the PV-LA junction may be crucial to promote re-entry formation and thus might play an important role as a substrate for the maintenance of AF. (J Am Coll Cardiol 2004;43: 2281–9) © 2004 by the American College of Cardiology Foundation

Atrial fibrillation (AF) can be triggered by focal activities in the pulmonary veins (PVs), and radiofrequency ablation of these foci can eliminate AF (1–3). Moreover, in patients with chronic AF and structural heart disease, after electrical cardioversion, the PVs are also the dominant trigger reinitiating AF (4). Therefore, the PVs may have an important role in not only the onset but also the maintenance of AF (5).

See page 2290

Previous studies have suggested that the PVs seemed to have the necessary substrate to support re-entry (6,7). In an animal study, the complete re-entrant loop in the PV has been visualized by high-resolution optical mapping (7). However, evidence of re-entry has not been demonstrated in humans. Moreover, the detailed electrophysiologic properties within the PV and at the PV–left atrial (LA) junction remain unclear. In this study, we used multielectrode basket catheter mapping to further define the electrophysiologic characteristics of the PV.

METHODS

Patients. The study population consisted of 48 patients (33 men and 15 women; mean age 56 ± 12 years) with symptomatic drug-refractory paroxysmal AF who were referred for an electrophysiologic study and catheter ablation. A mean of 3.0 ± 1.1 antiarrhythmic drugs had been administered unsuccessfully. No patients were treated with amiodarone during the six months preceding the procedure. The patients had frequent episodes of paroxysmal AF, frequent atrial premature beats documented by 24-h Holter monitoring, or spontaneous reinitiation of AF after defibrillation. Fourteen patients had additional cardiovascular diagnoses, including systemic hypertension (n = 11), ischemic heart disease (n = 2), and dilated cardiomyopathy (n = 1).

Electrophysiologic study. Written, informed consent was obtained from all patients. Patients were receiving oral anticoagulation at least one month before ablation. Antiarrhythmic drugs were discontinued at five half-lives before ablation. Three 6F quadripolar electrode catheters (Daig, Minnetonka, Minneapolis) were placed in the right atrial appendage, His bundle area, and coronary sinus (CS). A transseptal approach was performed with an 8.5F-long sheath for both the puncture and introducing the 31-mm, 64-pole basket catheter (EP Technologies, Sunnyvale, California) dedicated to PV mapping. A 4-mm-tip conventional ablation catheter (EP Technologies) was also introduced into the LA for ablation. Angiography of the PVs was performed with an angiocatheter (6F, Baxter, Deerfield, Illinois) to determine the position of a basket catheter relative to the ostium of the PVs. The proximal electrode (bipoles 7–8) of the basket catheter was located at the PV-LA junction. A catheter for the His bundle area was then introduced into the left atrial appendage (LAA) for stimulation purposes. The "proximal" part of the PVs was defined as the ostial side of the veins, whereas "distal" referred to the lung side of the veins.

From the Department of Cardiology, Fukuoka University Hospital, Fukuoka, Japan.

Manuscript received October 15, 2003; revised manuscript received January 8, 2004, accepted January 12, 2004.

Abbreviations and Acronyms

AF = atrial fibrillation
CS = coronary sinus
ERP = effective refractory period
LA = left atrium
LAA = left atrial appendage
LSPV = left superior pulmonary vein
PV = pulmonary vein
RSPV = right superior pulmonary vein

Stimulation protocol. Pulmonary vein pacing was performed from the distal (bipoles 1–2) or proximal (bipoles 7–8) electrode pair of all splines of the basket catheter. A programmed stimulator (SEC-3102, Nihon Kohden, Tokyo, Japan) was used to deliver electrical impulses of 2-ms duration at twice the diastolic threshold, the negative pole being connected to the distal electrode of the pacing catheter. Stable pacing sites were considered only if the threshold was <5 V. Electrocardiographic leads and intracardiac electrograms filtered at 30 to 500 Hz were recorded simultaneously with a polygraph (EPMed System, Century Medical, West Berlin, New Jersey). After a basic drive cycle of eight stimuli at a cycle length of 600 ms, a single extrastimulus coupled at 400 ms was decremented automatically in steps of 20 ms to the effective refractory period (ERP). The following variables were measured: 1) the ERP of the distal PV, PV-LA junction, or LAA was defined as the longest coupling interval at which a premature impulse failed to capture local muscle. 2) The conduction time from the distal PV to PV-LA junction or from the PV-LA junction to distal PV was measured from the pacing artifact to the atrial (S_1–A_1) or PV potential (S_1–PV_1) recorded during the drive cycle. 3) Conduction heterogeneity was defined as the difference between the minimum and maximum S_1–A_1 (or S_1–PV_1) among all the splines (Fig. 1). It was also measured at the shortest coupled extrastimulus propagated to the site (S_2–A_2 or S_2–PV_2). 4) Conduction delay was defined as the difference between the drive cycle conduction time and the conduction time of the shortest coupled extrastimulus propagated to the site (maximum S_2–A_2 or S_2–PV_2 minus maximum S_1–A_1 or S_1–PV_1, as in Fig. 1). 5) The electrical entrance breakthrough points during CS distal pacing (for left PVs) or sinus rhythm (for right PVs) and the exit breakthrough points during PV distal pacing were determined.

Activation mapping of PV during initiation of AF. Thirty-two bipolar electrograms obtained from a basket catheter during 12 episodes of induced AF and 10 episodes of spontaneous initiation of AF were analyzed. Conduction times from the earliest activation potentials or pacing artifact to each of the potentials were measured. For each beat, the activation time at each site was placed on an

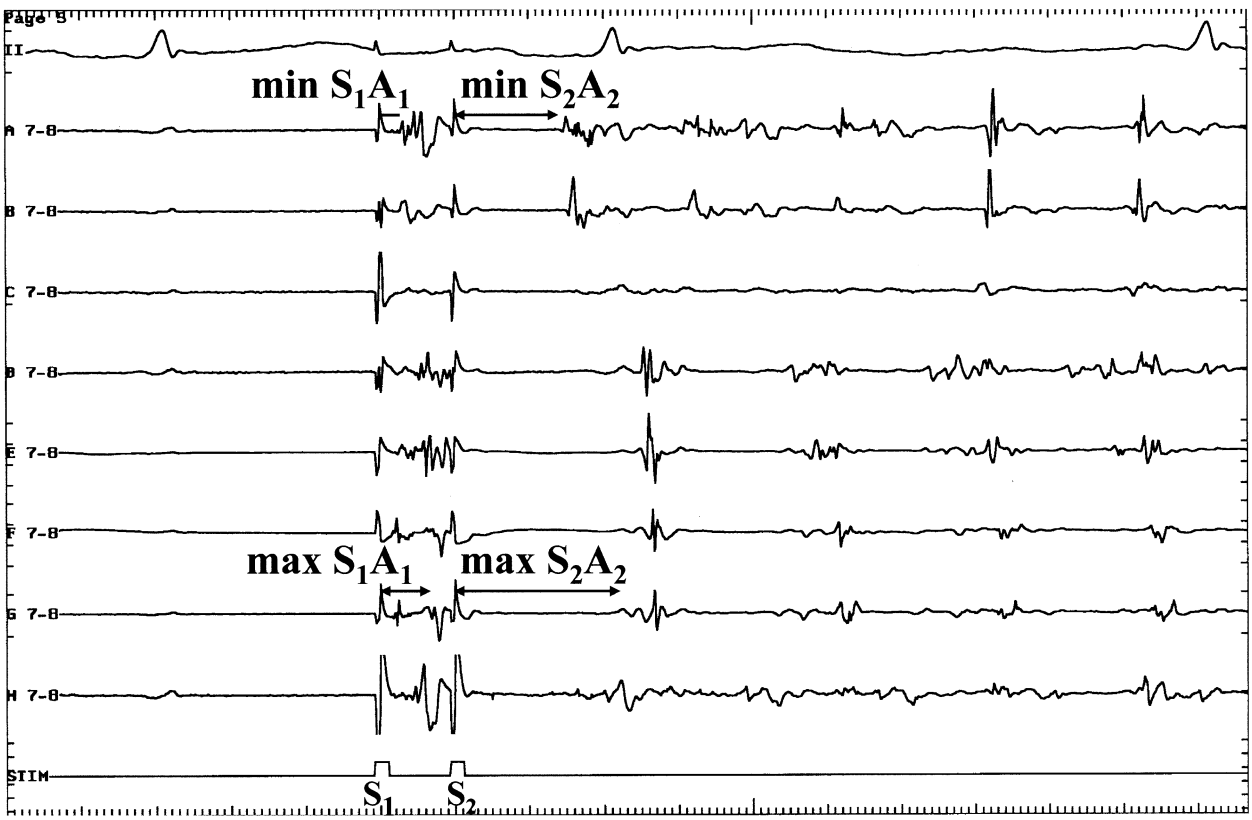

Figure 1. Electrophysiologic measurements. Proximal (bipoles 7–8) electrograms from all splines of the basket catheter placed in the left superior pulmonary vein are shown. The drive cycle conduction time (S_1–A_1) and the conduction time of the shortest coupled extrastimulus propagated to the site (S_2–A_2) are measured, and the minimum and maximum values among all the splines are determined. Letters **A to H** identify basket splines.

Table 1. Electrophysiological Parameters

Parameter	PV Distal Pacing	PV-LA Junctional Pacing	p Value
Threshold (V)	3.2 ± 0.5	3.1 ± 0.4	NS
ERP (ms)	177 ± 43	222 ± 30	< 0.0001
Min S_1–A_1/PV_1 (ms)	21 ± 8	23 ± 12	NS
Max S_1–A_1/PV_1 (ms)	40 ± 13	39 ± 14	NS
Min S_2–A_2/PV_2 (ms)	74 ± 32	51 ± 19	< 0.0001
Max S_2–A_2/PV_2 (ms)	114 ± 46	71 ± 19	< 0.0001
Conduction heterogeneity (ms)	41 ± 29	20 ± 11	< 0.0001
Conduction delay (ms)	73 ± 40	32 ± 17	< 0.0001

Data are presented as the mean value ± SD.
ERP = effective refractory period; LA = left atrial; Max = maximum; Min = minimum; PV = pulmonary vein.

anatomic grid representing activation at each bipolar recording site, and isochronous lines at 10-ms intervals were drawn manually. Analysis was based on sequential 100-ms time windows. For each episode, 600 ms of data (6 consecutive time windows) from initiation of the episode was analyzed, and the activation sequences were depicted by activation maps. When double potentials were recorded at the adjacent sites on either side of a line of functional block, depicted by dashed lines, local activation at each site was reflected by the large electrogram, and activation on the other side of the block by the low-amplitude potential. The area of slow conduction within a PV was identified as the region with crowding of isochrones.

Statistical analysis. Continuous variables are expressed as the mean value ± SD. Comparisons of electrophysiologic parameters between the pacing sites were calculated using the paired Student *t* test, and comparisons of parameters between the patients with and without induction of AF or re-entry were evaluated with the unpaired Student *t* test. Comparisons of the ratio of AF induction between the pacing sites were evaluated with the chi-square test. Statistical significance was set at $p < 0.05$.

RESULTS

Electrophysiologic parameters. Eighty-one PVs, including 42 left superior PVs (LSPVs) and 39 right superior PVs (RSPVs), were studied at 212 pacing sites. There was no significant difference in the threshold between the distal PV and PV-LA junction (Table 1).

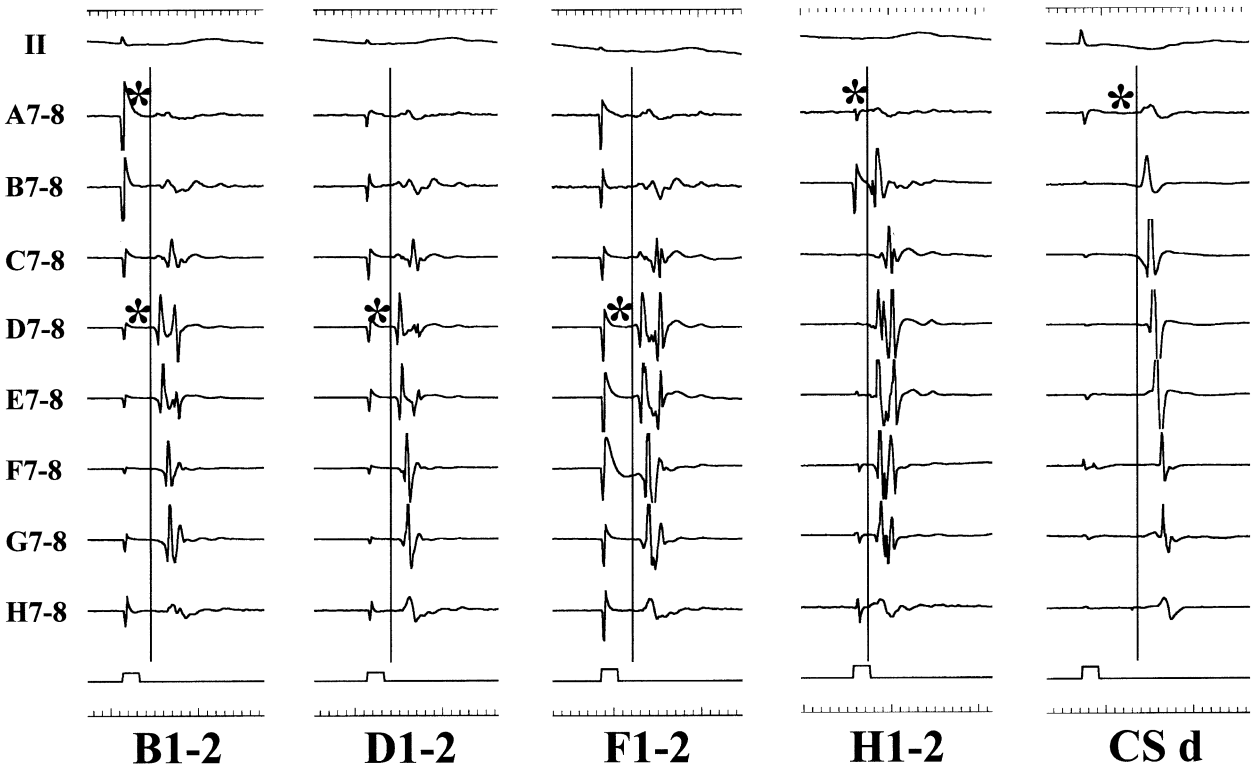

Figure 2. Detection of the exit breakthrough points by pulmonary vein (PV) distal pacing. Proximal (bipoles 7–8) electrograms from all splines of the basket catheter placed in the left superior pulmonary vein are shown. Of all PV distal pacing sites, four **(B, D, F, and H)** are shown. During pacing from **B1–2**, the earliest activation sites **(*)** are **A7–8** and **D7–8**. During pacing from **D** and **F1–2**, the earliest activation site **(*)** is **D7–8**. During pacing from **H1–2**, the earliest activation site **(*)** is **A7–8**. Thus, the exit breakthrough points are **A7–8** and **D7–8**. In contrast, during coronary sinus distal (CS d) pacing, the entrance breakthrough point **(*)** is **A7–8**.

JACC Vol. 43, No. 12, 2004
June 16, 2004:2281–9

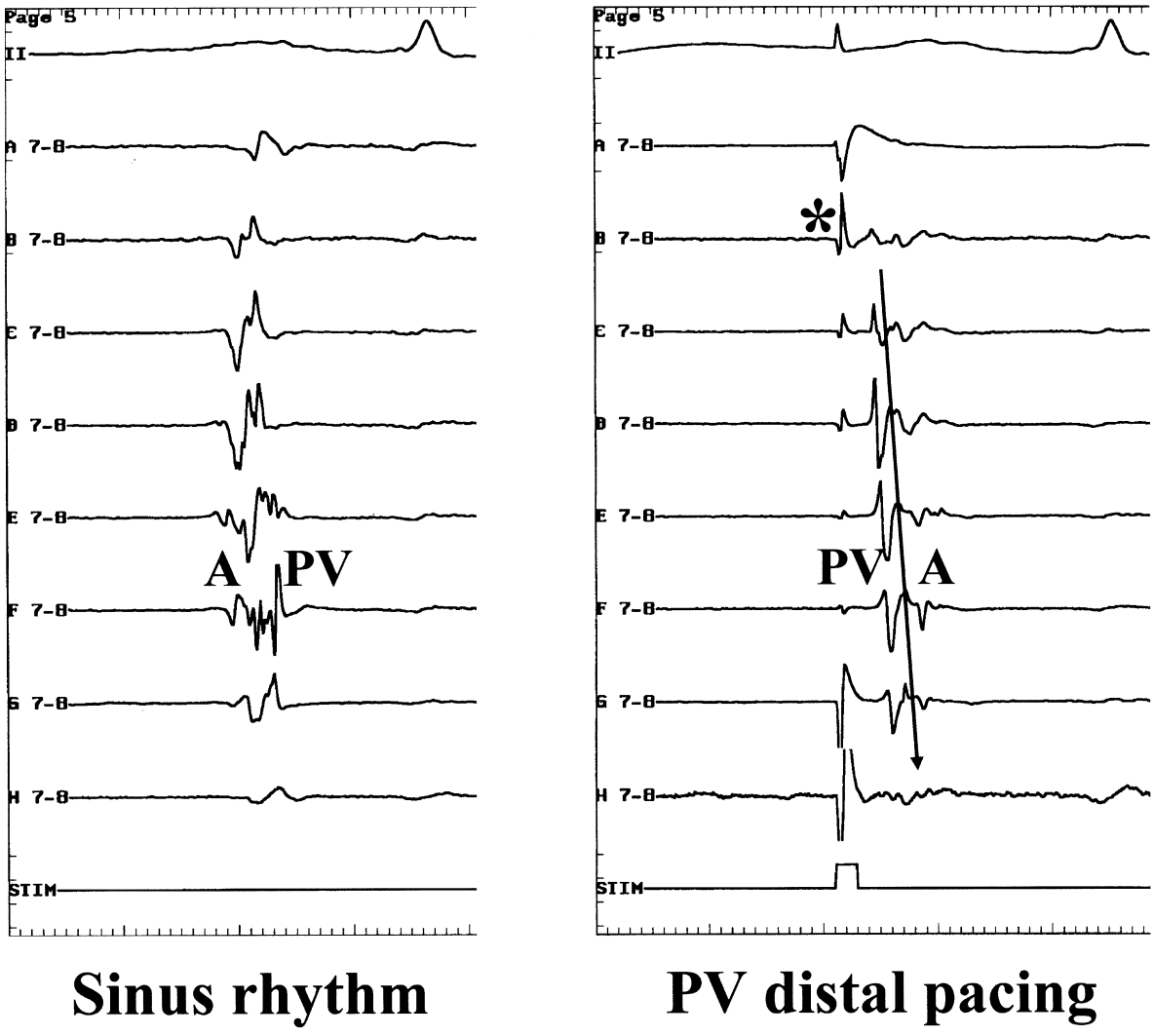

Figure 3. Detection of the exit breakthrough points in the right superior pulmonary vein (RSPV) by pulmonary vein (PV) distal pacing. Proximal (bipoles 7–8) electrograms from all splines of the basket catheter placed in the RSPV are shown. **(Left panel)** During sinus rhythm, atrial (A) and PV potentials approach each other. **(Right panel)** During PV distal pacing from A 1–2, these potentials are discriminated. The exit breakthrough point **(*)** is **B 7–8**.

The ERPs of distal PVs (mean 177 ± 43 ms [range 60 to 280]) were significantly shorter than those of the PV-LA junction (mean 222 ± 30 ms [range 160 to 280]) or LAA (mean 215 ± 25 ms [range 180 to 260]). There were no significant differences in the ERPs between the PV-LA junction and LAA. Dispersion of ERP, defined as the difference between the minimum and maximum ERP within the same PV, was 46 ± 35 ms.

The conduction time from the distal PV (bipoles 1–2) to PV-LA junction (bipoles 7–8) was significantly longer than that from the PV-LA junction to distal PV when pacing was performed at the same spline (42 ± 15 vs. 33 ± 14 ms, $p < 0.0001$). However, there were no significant differences in the minimum and maximum conduction times during the drive cycle between S_1–A_1 and S_1–PV_1 (Table 1). The conduction time at the shortest coupled extrastimulus, the conduction heterogeneity, and the maximum conduction delay from the distal PV to PV-LA junction were significantly longer than those from the PV-LA junction to distal PV (Table 1).

Atrial fibrillation was more frequently induced when a single extrastimulus was performed in distal PVs versus the PV-LA junction (12% vs. 1%, $p < 0.01$). The patients with AF induction had a significantly shorter ERP of distal PVs (156 ± 65 vs. 184 ± 33 ms, $p < 0.05$) and a longer conduction delay from the distal PV to PV-LA junction (97 ± 42 vs. 64 ± 36 ms, $p < 0.01$) than those without AF induction. However, there were no significant differences in the ERPs of the PV-LA junction, the conduction heterogeneity in bidirections, and the conduction delay from the PV-LA junction to distal PV between the patients with and without AF induction.

Figure 2 presents the exit breakthrough points of a LSPV disclosed by PV distal pacing. In this case, during CS distal pacing, the entrance breakthrough site was A 7–8. In contrast, two exit breakthrough points were detected at A 7–8 and D 7–8. These exit breakthrough points were targeted for the segmental PV isolation. Figure 3 shows the electrograms around the PV-LA junction of a RSPV. In this case, during sinus rhythm, the PV and LA potentials approach each other.

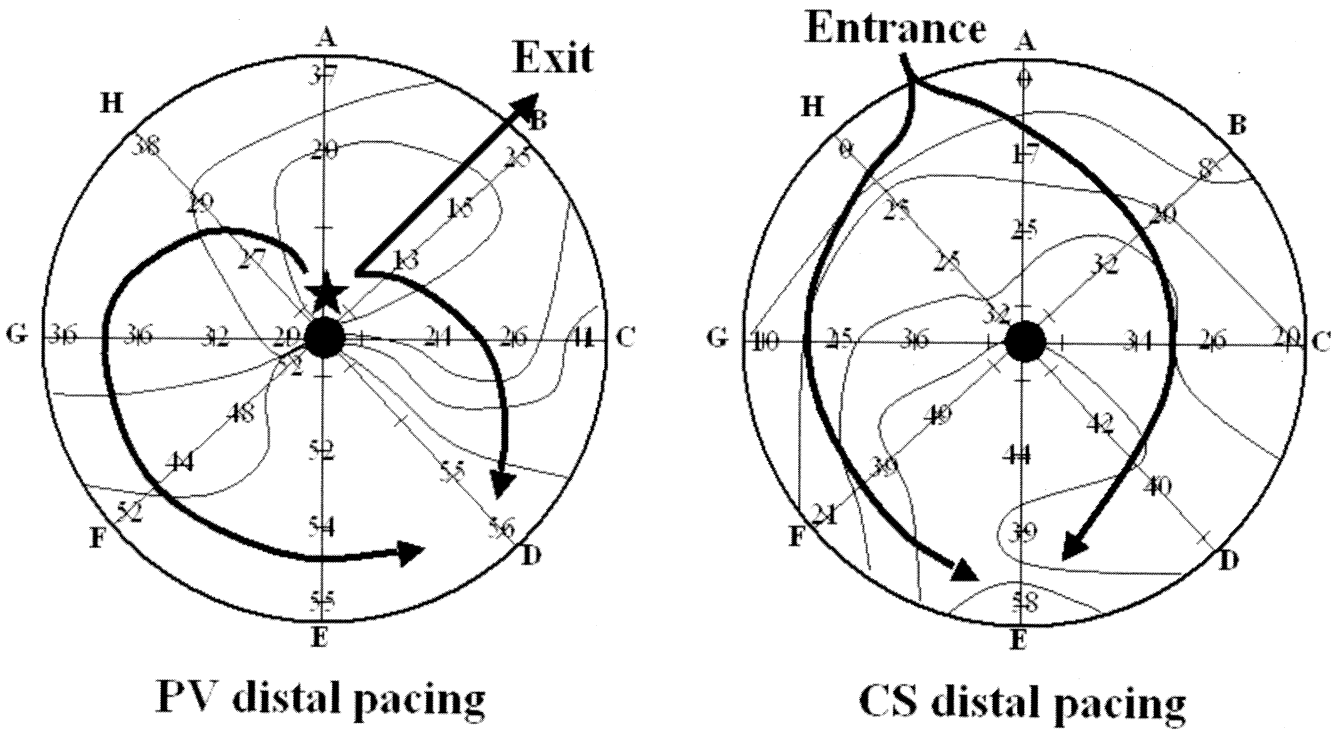

Figure 4. Activation maps of the left superior pulmonary vein during pulmonary vein (PV) distal pacing and during coronary sinus (CS) distal pacing from a representative episode. Letters **A to H** identify basket splines. An anatomic grid is shown in an apical view, with the distal electrodes in the center and proximal electrodes on the periphery. **Lines with arrows** indicate activation wave fronts. **Thin lines** represent isochrones at 10-ms intervals. **(Left map)** During PV distal pacing from bipoles **A 1–2 (star)**, the earliest activation site around the PV-left atrium junction (i.e., the exit breakthrough point) is **B 7–8**. **(Right map)** During CS distal pacing, the entrance breakthrough point is **A** or **H 7–8**.

However, the distal PV pacing discriminated between these potentials and disclosed the exit breakthrough point.

Analysis of consecutive activation patterns during initiation of AF induced by extrastimulation. Figure 4 shows activation maps of a LSPV during PV distal pacing and during CS distal pacing from a representative episode. During PV distal pacing from bipoles A 1–2, the earliest activation site around the PV-LA junction (i.e., the exit breakthrough point) is B 7–8 (Fig. 4, left panel). In contrast, during CS distal pacing, the entrance breakthrough point is A or H 7–8 (Fig. 4, right panel).

Figure 5A presents consecutive activation maps from this episode of initiation of AF induced at a coupling interval of 200 ms during distal PV pacing from bipoles A 1–2 at a cycle length of 600 ms. In Figure 5B, window 1 shows that the impulse from the pacing site was blocked in A 5–6 and went from the PV to LA at splines B and C 7–8, where there is an exit breakthrough point. In window 2, a wave front coming from LA reentered the PV at H 7–8 and bifurcated. A branch of these wave fronts was blocked in the E area at 126 ms, and another branch was also blocked in the E area at 240 ms (window 3). A new wave coming from the LA entered the PV from E 7–8 (window 4). A branch of the bifurcated wave front went around a functional block line and disappeared in the D area, colliding with another branch at 400 ms. After 400 ms, no electrical activity was seen in the entire PV until a new wave front from E 7–8 entered the PV again at 495 ms (window 5). A branch of the bifurcated wave front entered the PV and collided with a branch of new wave coming from A 7–8 at 526 ms, finally disappearing in the D area (window 6). Thus, in this case, a PV-LA reciprocating re-entrant circuit involving the exit and entrance breakthrough points was observed at the start of AF. Wave fronts traveling to and from the LA may play an important role in the reformation of activation.

Analysis of consecutive activation patterns during spontaneous onset of AF. Figure 6 shows an episode of spontaneous onset of AF from F 5–6 in a RSPV. In window 1, a focal discharge occurred from F 5–6, and two wave fronts collided with each other and disappeared in the A area. A second focal activity occurred from the same site again, but wave fronts were blocked in the PV (window 2). A third discharge occurred from F 7–8, and two wave fronts collided with each other and went to the A-B area (window 3). These wave fronts went out of the PV at 300 ms, went around the PV-LA junction, and re-entered the PV from F 7–8 at 323 ms, forming a re-entrant circuit (window 4). A branch of wave was unidirectionally blocked between G and H, but another branch went around the PV, forming a re-entrant circuit in the PV (window 4). This re-entrant circuit lasted for 1.5 rotations, had a cycle length of 100 ms (windows 4 through 6), and was blocked in the G area at 514 ms (window 6). A branch of this re-entrant circuit went out of the PV at 500 ms (window 5), went around the PV-LA junction, and reentered the PV from F 7–8 at 536 ms (window 6). Then, an activation pattern similar to that

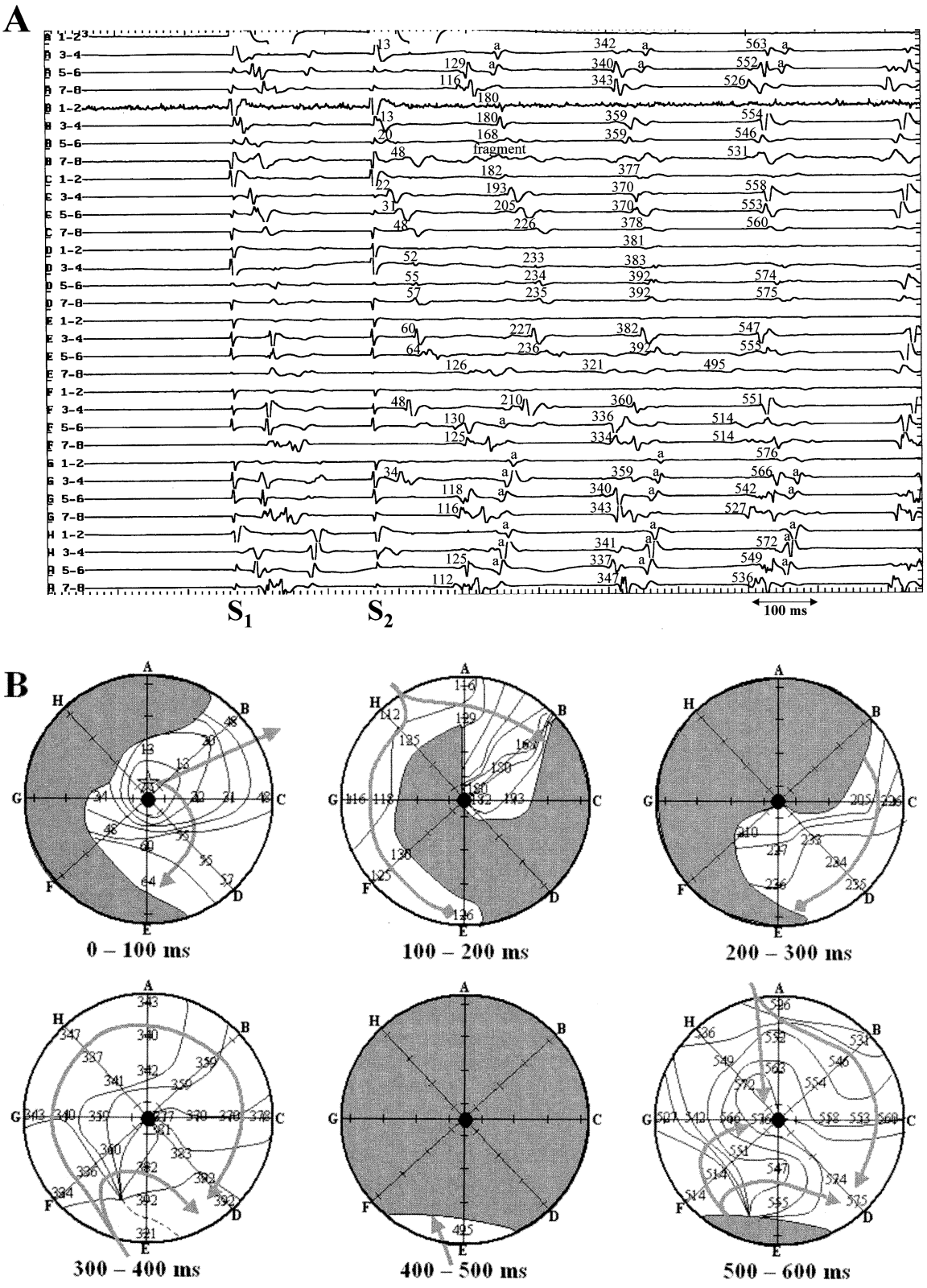

Figure 5. Analysis of consecutive activation patterns during a representative episode of initiation of atrial fibrillation (AF) induced by extrastimulation from **A 1–2**. **(A)** Pulmonary vein recordings from a basket catheter placed in the left superior pulmonary vein from the same patient as shown in Figure 4. After extrastimulus S_2 of 200 ms, AF is induced. The **numbers** identify the conduction times from S_2. a = far-field atrial potential. **(B)** A total of 600 ms of data (six consecutive time windows) from an initiation of the episode is analyzed. The **star** indicates the pacing site **(A 1–2)**. **Dark gray regions** indicate areas that were not activated during a 100-ms window. The **dashed line** indicates a line of functional block. In this case, a re-entrant circuit involving the exit breakthrough point (splines B and C) and the entrance breakthrough point (spline H) starts AF. Wave fronts traveling to and from the left atrium may play an important role in reformation of activation. However, no re-entrant circuits only within the pulmonary vein are observed.

in window 4 was observed (window 6). Thus, in this case, rapid, repetitive firings in a PV induced the PV-LA conduction block and PV-LA reciprocating re-entrant circuit involving the exit breakthrough point, and the entrance breakthrough point was created. Also, a re-entrant circuit within the PV was observed; however, this re-entry was unstable and short-lived.

Similar activation patterns were also observed in other cases, although there were minor differences between them. For example, in eight cases, no re-entrant circuit within the PV was seen. However, re-entrant circuits lasting for more than two rotations were never observed in any cases. The patients with re-entry had a significantly shorter ERP of distal PVs (127 ± 60 vs. 199 ± 37 ms, $p < 0.01$), a longer conduction heterogeneity (60 ± 43 vs. 30 ± 15 ms, $p < 0.01$), and a longer conduction delay from the distal PV to PV-LA junction (110 ± 51 vs. 72 ± 25 ms, $p < 0.01$) than those without re-entry. However, there were no significant differences in the ERPs of the PV-LA junction, conduction heterogeneity, and conduction delay from the PV-LA junction to distal PV between the patients with and without re-entry.

DISCUSSION

The present study has demonstrated, using basket catheter mapping, distinct electrophysiologic characteristics of PVs and the PV-LA junction in patients with AF. The findings can be summarized as follows: 1) the ERP of the distal PV was significantly shorter than that of the PV-LA junction; 2) the conduction delay from the distal PV to PV-LA junction was significantly longer than that from the PV-LA junction to distal PV; and 3) during initiation of AF, a short coupled extrastimulus or rapid, repetitive focal activities originating from the PV formed a PV-LA reciprocating re-entrant circuit involving exit and entrance breakthrough points at the PV-LA junction.

Programmed stimulation showed that distal PV ERPs are significantly shorter than PV-LA junctional ERPs and LAA ERPs. The ERPs of the PV-LA junction and the LA are comparable. Chen et al. (3) reported that the ERPs of the distal PV were significantly shorter than those of the proximal PV, but not significantly different from atrial ERPs. In contrast, Jaïs et al. (6) recently reported that the PV ERPs were significantly shorter than those of the LA, and extremely short PV ERPs were observed, consistent with the results of the present study.

The other significant finding of the present study is the pronounced conduction abnormality seen in PVs. The decremental conduction properties of PVs in humans have been demonstrated by Jaïs et al. (6); however, they did not compare differences in the conduction properties between the directions of activity. In the present study, the conduction time, conduction heterogeneity, and maximum conduction delay from the distal PV to PV-LA junction were significantly longer than those from the PV-LA junction to distal PV. These conduction properties could therefore be related to anisotropic conduction (8), with the fractionated venous potentials and associated changes in activation sequence and exits probably correlating with the complex arrangement of venous muscular sleeves (9). Thus, the significant differences in the electrophysiologic properties between the PV and PV-LA junction provide a very favorable characteristic for re-entry within or around the PVs, which may perpetuate arrhythmia and thus act as a substrate for AF maintenance.

In animal studies, Arora et al. (7) demonstrated that nonsustained re-entrant beats were induced with a single extrastimulus, and the complete re-entrant loop was visualized using high-resolution optical mapping. This re-entry was consistent with the classic "leading-circle" model, in that it seemed to occur in the absence of an anatomic obstacle (i.e., functional re-entry) (7). However, there was no evidence of re-entry within or around the PVs in humans. In the present study, unstable re-entrant circuits were observed in response to a single extrastimulus and repetitive focal activities in the PV. When a coupling interval of extrastimulus or the cycle length of repetitive focal activities is so short, the rest of the PV cannot follow 1:1. The result is that areas of functional block and slow conduction are generated, which in turn serve to form an unstable re-entrant circuit. However, these re-entrant circuits were short-lived and never sustained for more than two rotations (i.e., unstable).

Moreover, as shown in the maps during initiation of AF (windows 1 and 2 in Fig. 5B and windows 3 and 4 in Fig. 6B), a PV-LA reciprocating re-entrant circuit involving the exit breakthrough point and the entrance breakthrough point at the PV-LA junction was observed. A wave front from a focal discharge in the PV goes through the nearest exit breakthrough point and reenters the PV from the entrance site, forming a re-entrant circuit. The different conduction property of the exit and entrance sites, depending on the site of pacing or discharge, may contribute to the re-entry formation. Wave fronts traveling to and from the LA may play an important role in the formation of unstable re-entrant wave fronts. In the study by Hamabe et al. (10) of canine PVs, histologic sections at the PV-LA junction with conduction block showed the presence of abrupt changes in myocardial fiber orientation. The complex arrangement of myocardial fibers at the PV-LA junction is a possible reason for conduction delay or block in the PV-LA junction (11–14). The presence of anisotropic structures at the PV-LA junction may be crucial to form re-entry.

Study limitations. A limitation of our study is the fact that we had relatively poor recording resolution. We used 32 bipolar electrodes to record from the PV. Clearly, this may be a less-than-optimal recording resolution. However, in humans, this is the highest recording resolution of endocardial mapping by a catheter so far. The size of the basket catheter was relatively small for the PV; therefore, the basket splines closely approach each other, improving the resolution. We demonstrated a reciprocating circuit at the

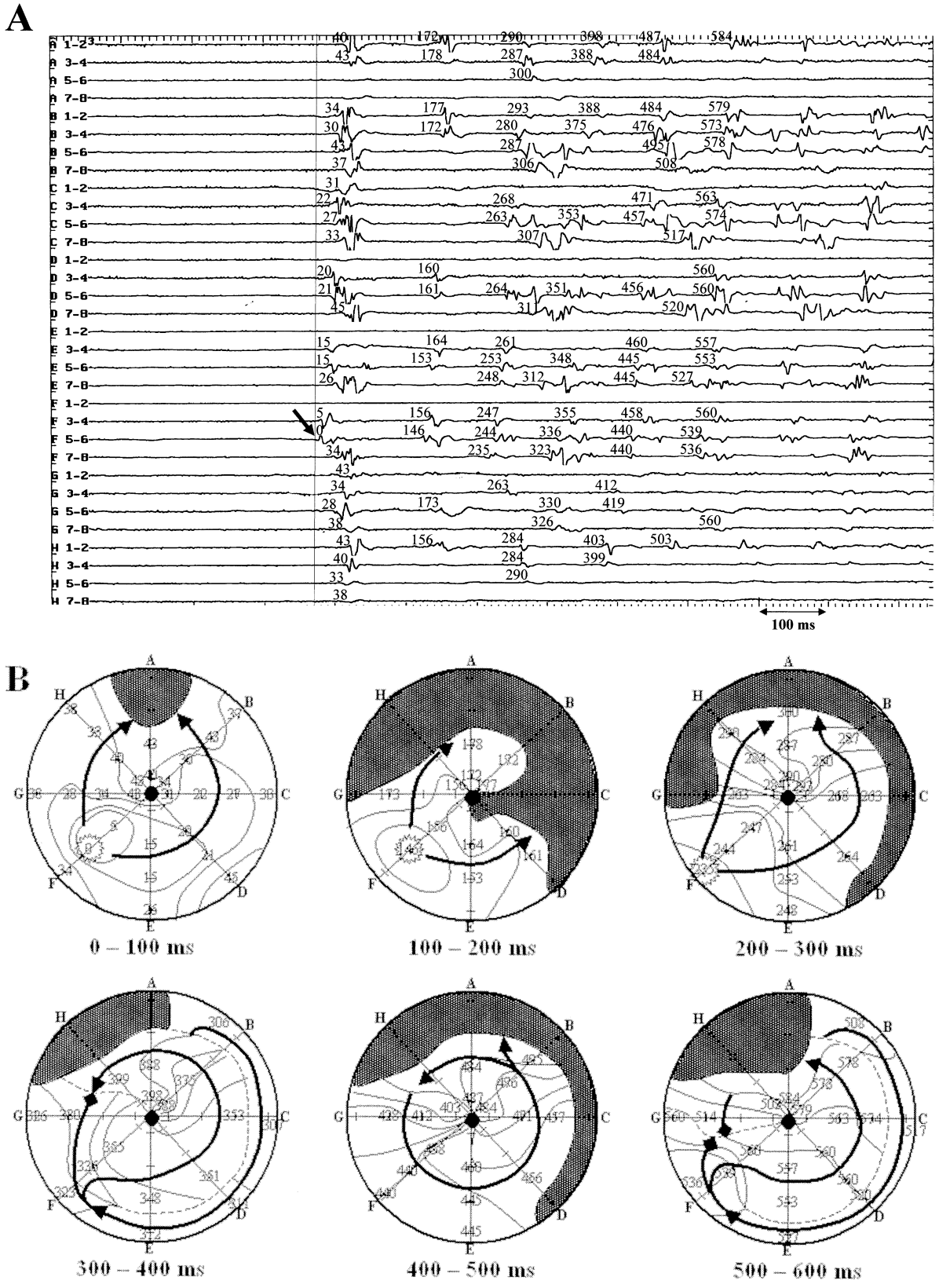

Figure 6. Analysis of consecutive activation patterns during a representative episode of spontaneous onset of atrial fibrillation (AF). **(A)** Pulmonary vein recordings from a basket catheter placed in the right superior pulmonary vein during an episode of spontaneous onset of AF from **F 5–6**. The **numbers** identify the conduction times from the earliest activation potential. **(B)** In this case, rapid, repetitive firings induce the pulmonary vein (PV)-left atrium (LA) conduction block and PV-LA reciprocating re-entrant circuit involving the exit breakthrough point (splines A and B), and the entrance breakthrough point (spline F) is created. Also, a re-entrant circuit lasting for 1.5 rotations, with a cycle length of 100 ms, is observed within the PV.

PV-LA junction, but it does not prove that AF is induced by this circuit, or that activation of the vein is crucial or necessary to maintain re-entry, because no recordings were made in the whole atria. However, the presence of re-entry within the PV and at the PV-LA junction is the unique finding of this study.

Reprint requests and correspondence: Dr. Koichiro Kumagai, Department of Cardiology, Fukuoka University Hospital, 7-45-1, Nanakuma, Jonan-ku, Fukuoka 814-0180, Japan. E-mail: kxk@fukuoka-u.ac.jp.

REFERENCES

1. Jaïs P, Haïssaguerre M, Shah DC, et al. A focal source of atrial fibrillation treated by discrete radiofrequency ablation. Circulation 1997;95:572–6.
2. Haïssaguerre M, Jaïs P, Shah DC, et al. Spontaneous initiation of atrial fibrillation by ectopic beats originating in the pulmonary veins. N Engl J Med 1998;339:659–66.
3. Chen SA, Hsieh MH, Tai CT, et al. Initiation of atrial fibrillation by ectopic beats originating from the pulmonary veins: electrophysiological characteristics, pharmacological responses, and effects of radiofrequency ablation. Circulation 1999;100:1879–86.
4. Haïssaguerre M, Jais P, Shah DC, et al. Catheter ablation of chronic atrial fibrillation targeting the reinitiating triggers. J Cardiovasc Electrophysiol 2000;11:2–10.
5. Kumagai K, Yasuda T, Tojo H, et al. Role of rapid focal activation in the maintenance of atrial fibrillation originating from the pulmonary veins. Pacing Clin Electrophysiol 2000;23:1823–7.
6. Jaïs P, Hocini M, Macle L, et al. Distinctive electrophysiological properties of pulmonary veins in patients with atrial fibrillation. Circulation 2002;106:2479–85.
7. Arora R, Verheule S, Scott L, et al. Arrhythmogenic substrate of the pulmonary veins assessed by high-resolution optical mapping. Circulation 2003;107:1816–21.
8. Spach MS. Anisotropy of cardiac tissue: a major determinant of conduction? J Cardiovasc Electrophysiol 1999;10:887–90.
9. Ho SY, Sanchez-Quintana D, Cabrera JA, et al. Anatomy of the left atrium: implications for radiofrequency ablation of atrial fibrillation. J Cardiovasc Electrophysiol 1999;10:1525–33.
10. Hamabe A, Okuyama Y, Miyauchi Y, et al. Correlation between anatomy and electrical activation in canine pulmonary veins. Circulation 2003;107:1550–5.
11. Nathan H, Eliakim M. The junction between the left atrium and the pulmonary veins: an anatomic study of human hearts. Circulation 1966;34:412–22.
12. Saito T, Waki K, Becker AE. Left atrial myocardial extension onto pulmonary veins in humans: anatomic observations relevant for atrial arrhythmias. J Cardiovasc Electrophysiol 2000;11:888–94.
13. Ho SY, Cabrera JA, Tran VH, et al. Architecture of the pulmonary veins: relevance to radiofrequency ablation. Heart 2001;86:265–70.
14. Hocini M, Ho SY, Kawara T, et al. Electrical conduction in canine pulmonary veins: electrophysiological and anatomic correlation. Circulation 2002;105:2442–8.